Modeling of the Organ of Corti Stimulated by Cochlear Implant Electrodes and Electrodes Potential Definition Based on their Part inside the Cochlea

Umberto Cerasani and William Tatinian
University Nice Sophia Antipolis
LEAT UMR CNRS-UNS 6071
Valbonne, France
Email :
umberto.cerasani@unice.fr william.tatinian@unice.fr

***Abstract* – Cochlear implants are used by deaf people to recover partial hearing. The electrode array inserted inside the cochlea is an extensive area of research. The aim of the electrodes array is to directly stimulate the nerve fibers inside the Organ of Corti. The electrical model of the physical system consisting of Organ of Corti and the electrodes is presented in this paper. This model allowed to run SPICE simulations in order to theoretically detect the minimal voltage sufficient for nerve fiber stimulation as well as the impact of the electrode voltage on the duration of nerve fibers stimulation. Besides, to ensure functional sound perception, the electrode potential should depend on their position inside the cochlea. A afferent nerve fiber repartition map over the cochlea position, considering the frequency sensitivity of the different parts of the ear was created. This projection allowed to propose a theoretical electrodes potential correction based on their cochlea position.**

Keywords: cochlear implant, electrical analog, transient simulations, afferent nerve fibers repartition, spiral ganglions

I. INTRODUCTION

Cochlear implants are an electrical device used by severely deaf people to gain or recover partial audition. They allow direct stimulation of the auditory fibers using an electrodes array designed to reproduce the stimulus that would be generated by a healthy cochlea.

To do so, an external part of the hearing devices is located outside the ear and contains a microphone that captures the acoustic waves and transforms them into an electrical signal used by the data processing unit. Then, this signal is transmitted to the receiver, located within the patient's head, close the skull. The receiver is composed of a demodulator and a set of electrodes driven by electrical signals that will contract the cochlea and stimulate the auditory nerve [1], [2], [3].

Cochlear implants directly stimulate the nerve fibers inside the cochlea, and requires surgery to pull the electrodes array inside the scala tympani (Figure 1).

The connection between the electrodes in the scala tympani and the auditory nerve fibers is critical for efficient nerve fibers stimulation.

In an healthy ear, when a sound wave is produced, it strikes the eardrum and this vibration is reported in the oval window using ossicles. The oval window is the very first part of the cochlea. This oval window vibration creates a wave propagating inside the scala vestibuli, which is filled with perilymph.

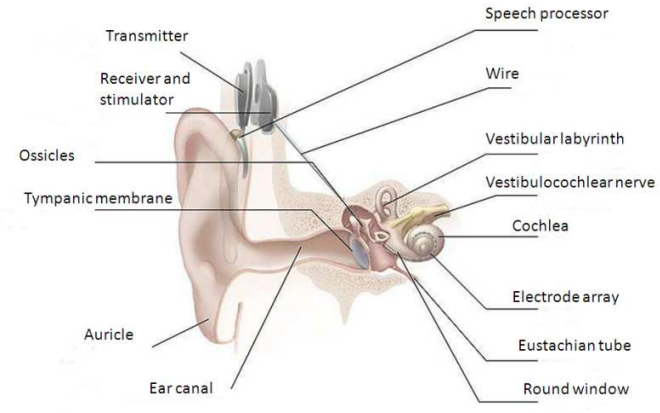

Figure 1. Cochlear implant device [3]

According to biophysical theories [4], [5] when a mechanical wave propagates inside the cochlea, the Basilar Membrane (BM) distorts to absorb the wave energy, resulting in a height variation of the BM, which compresses the organ of Corti. As shown in Figure 2, the organ of Corti is composed of Hair Cells (HC) (Outer Hair Cells (OHC) and Inner Hair Cells (IHC)), which have stereocilia at their end. When BM vibrates, stereocilia position change allowing potassium channels to open [6, 7]. Opening of the potassium channels creates the depolarization of the HC allowing complex mechanisms to take place (reviewed in [8], [9], [10]), and finally, resulting in neurotransmitter released in the synapse. Once released, these neurotransmitters travel to the post synaptic cell (the nerve fiber) and creates the depolarization of the nerve fiber. This depolarization, if sufficiently important, generates an Action Potential (AP) running through the nerve cell membrane [11], [12].

The aim of the electrodes array of the cochlear implant is to generate an AP once a sound is perceived.

2014, © Copyright by authors, Published under agreement with IARIA - www.iaria.org

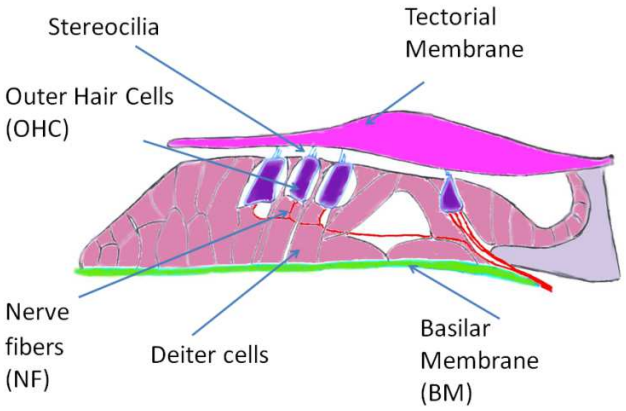

Figure 2. Organ of Corti

Consequently, to obtain the same Action Potential at the nerve fiber using only electrode stimulation, two possibilities exist. First the direct nerve fiber stimulation can be made by changing the nerve membrane potential in order to produce a membrane depolarization above the threshold of Voltage Sensitive Na+ Channels (Na_v) to create an AP [13]. The second solution consists in opening the potassium channels of the stereocilia to recreate the complete stimulation process. As HC or stereocilia are disfunctionning in the vast majority of implanted patients, only the first mechanism is considered in this paper.

Electrical model of electrodes inserted within the cochlea have been proposed by Hartmann et al. [14], where the spatial distribution of electrical potential was measured for intracochlear stimulation. In addition, electronic model of electrode/neuron coupling is available in [15] in order to reveal the most efficient coupling conditions. However, both models lack of physical connection with AP generation. In this paper, we present an electrical description of the electrode and organ of Corti in order to obtain theoretical minimal stimulation voltage sent to the electrodes for AP generation. Furthermore, this model allowed us to link the stimulation voltage with the duration of the nerve fibers stimulation. Then the impact of surrounding electrodes were theoretically investigated.

The next section presents the theoretical model developed for the Organ of Corti associated with the electrodes. Thereafter, simulation results from SPICE software are presented.

The threshold of hearing [16] describes the minimum power of the acoustic vibration required to perceive a sound related to the sound frequency. This relation is not linear for mammals, indicating that various physical properties of the ear ensure this frequency selectivity. As the Central Nervous System (CNS) interprets the message sent by the afferent nerve fibers, this frequency selection has to be recreated in cochlear implants where the afferent nerve fibers are directly stimulated. In that intent, we used two topographic maps of the cochlea: one describing the repartition of the afferent nerve fibers (also called Spiral Ganglion Cells (SGC) (cf Section V)) over their place inside the cochlea and another one describing the same repartition but weighted by a threshold of hearing related function. By comparing the number of afferent nerve cells stimulated in both maps, we defined corrective coefficients. These coefficients were used to correct the potential sent to the electrodes and may permit better sound reconstruction by the brain.

Finally, the conclusion and future work direction are presented.

II. ORGAN OF CORTI ELECTRICAL ANALOG

The electrical equivalent circuit of human tissue used in this paper is the one presented in Figure 3 and extracted from Cole and Cole impedance model [17], which has been shown to fit experimental data. The human tissues considered were the one present in Figure 2. The value of R_s, R_p , C_h and C_p were obtained using a gain response extraction over frequencies analysis.

The electrical analog model is based on the impedance response over frequencies. R_s and C_h model the tissue impedance at low frequencies. As the maximum hearing frequency is 22khz, it was considered in this paper that R_p and C_p could be neglected as their model the energy loss and tissue response in high frequencies.

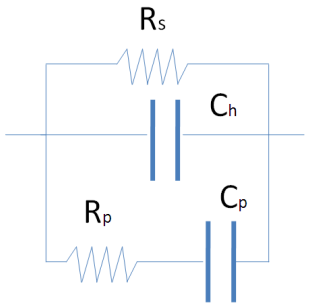

Figure 3. Human tissue electrical analog [17]

To obtain the numerical values for R_s and C_h for all the tissues or interfaces, we use the physical equations for the capacitance (parallel-plate capacitor) and for the resistance computation (cylindrical resistance model) [18], [19].

The values of the relative permeability and electrical conductivity for the nerves were extracted from [20] or from [21] for platinum as electrodes are mainly composed of it. However as far as the authors know, no relative permeability or electrical conductivity was available for Deiter cells or Basilar Membrane tissue. As Deiter cells are mainly composed of microtubules [22], which are involved in mechanical transport as actin proteins found in muscles cells and because the width of the BM is negligible compared to the Deiter cell height, we chose to take the relative permeability and electrical conductivity of muscle cells to characterize those two tissues.

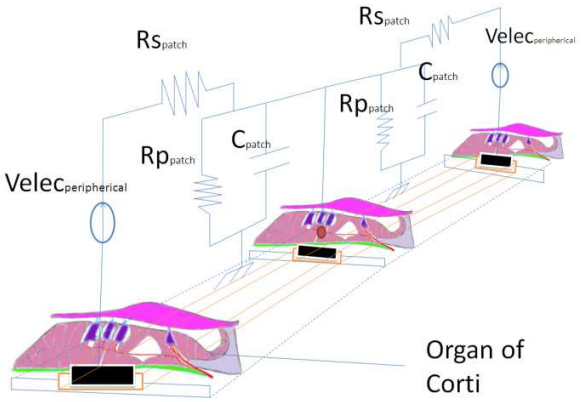

Figure 4. Two surrounding electrodes influences the nerve fibers targeted.

2014, © Copyright by authors, Published under agreement with IARIA - www.iaria.org

On the other hand, the computation of the capacitance and the resistances (C_{patch}, Rp_{patch}, Rs_{patch}) between two electrodes is more complex, as highlighted Figure 4, those variables depend on the distance between the two electrodes. The Cable Model Theory was used to compute those variables as the space between two electrodes is composed of various tissues rendering the Cole and Cole model implementation difficult. We simplified the tissue between two electrodes as only made of Deiter cells, then we implemented the Cable Model Theory in order to obtain a general impedance depending on the electrodes distance.

To compute Rs_{patch}, the cylindrical model of resistance was considered. The cylinder going from the first electrode to the second electrode, as defined in Figure 5.a, was used to compute Rs_{patch} (expressed in (1)):

$$R_{spatch} = \frac{1}{\sigma_M} * \frac{l_{spatch}}{S_{spatch}}$$

$$\text{with} \quad l_{spatch}(y) = \int_0^{Y_{tot}} y * dy$$

$$\text{and} \quad S_{spatch}(y) = \int_0^{2*\pi} \int_{-\frac{X1}{2}}^{\frac{X1}{2}} \rho * d\rho * d\theta \qquad (1)$$

where σ_M is the electrical conductivity of muscle cells, Y_{tot} is the distance between the two electrodes, X_1 is the distance between one electrode and the corresponding nerve fibers. Those values were respectively extracted from [23] and [24]. y is the variable shown in Figures 5.a, 5.b and 5.c.

Rp_{patch} models the resistance between the two longitudinal edges of the cylinder defined previously. Hence, this computation changes as expressed in (2), as it models all the losses through the ground from one electrode to another one.

$$R_{ppatch} = \frac{1}{\sigma_M} * \frac{l_{ppatch}}{S_{ppatch}}$$

$$\text{with} \quad l_{ppatch}(y) = \int_0^{Z1} dz$$

$$\text{and} \quad S_{spatch}(y) = \int_0^{2*\pi} \int_0^{y} \rho * d\rho * d\theta \qquad (2)$$

where Z_1 is the distance between the electrode and the nerve fibers and we supposed Z_1 equal to X_1 for simplification purposes.

We defined Cp_{patch} as a squared parallel plate capacity (Figure 5.c) (developed in (3)):

$$C_p = \mathcal{E}_0 \mathcal{E}_M \frac{A_{patch}}{d_{patch}}$$

$$\text{with} \quad d_{patch}(y) = \int_0^{Z_1} dz$$

$$\text{and} \quad A_{patch}(y) = \int_0^{y} dy_1 \int_0^{X_1} dx \qquad (3)$$

Where $\mathcal{E}_0$ is the vacuum permeability and $\mathcal{E}_M$ is the muscle relative permeability.

For reader's convenience, the value of the capacitance and resistance described previously are summarized in Table I.

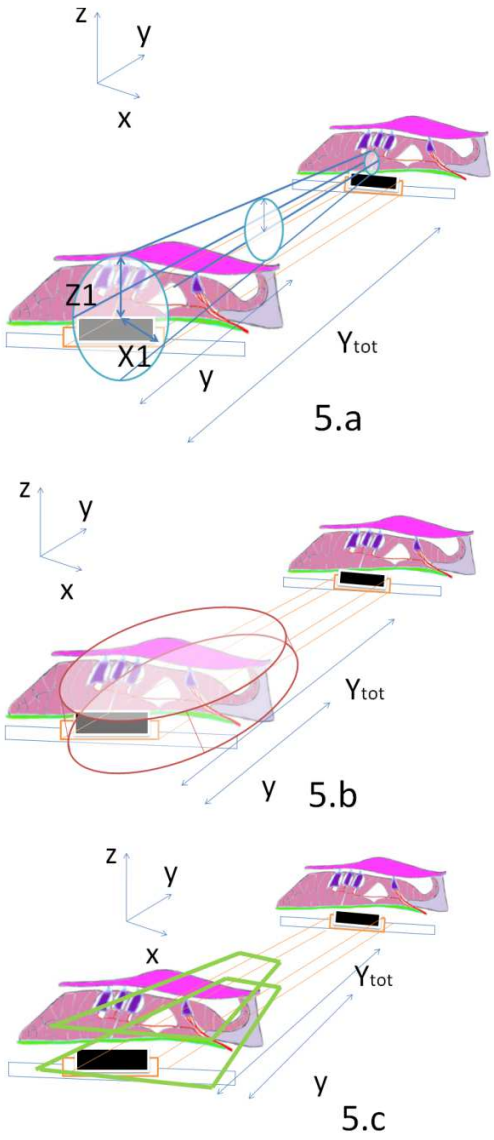

Figure 5. Physical model of Rs_{patch} (5.a), Rp_{patch} (5.b) and Cp_{patch} (5.c)

The electrical description containing only a single electrode is shown Figure 6.a. The input voltage generator is directly connected to the electrodes analog model (low frequencies model), which can be eventually considered as a perfect conductor compared to the other resistance values. Then the current can flow to the nerve cell or can go back to the ground. The current loss through the physical isolation between the electrode and the ground is neglected as the insulator has a low loss tangent (high resistivity). The membrane rest potential of a nerve cell is around -70mV, explaining the two -70mV voltage generators, in Figure 6.a. We defined the analog equivalent circuit of a nerve cell using a resistance (R_n) in parallel with a capacitor (C_n) (this electrical description should not be confused with the Hodgkin-Huxley model [25], which is used to model ions flow through the nerve cell membrane and not the electron flow).

In addition, the electrical description of the system starting from the nerve and going through all the body to the earth was not considered because very little electrical current is going through this pathway.

2014, © Copyright by authors, Published under agreement with IARIA - www.iaria.org

TABLE I. RESISTANCES AND CAPACITANCES USED IN THE ELECTRICAL MODEL

Electrodes	**Re= 1.5 Ω, Ce=11 fF**
Basilar Membrane and Deiter cells	R_{bc}= 933 Ω, C_{bc}= 300 nF
Nerve fibers	R_n= 1076Ω, C_n= 3µF
Cable Model Theory	Rs_{patch}= 8 MΩ, Rp_{patch}= 1265 Ω Cp_{patch}= 92.6 nF

Figure 6.b exhibits the electrical description of the overall system with two surrounding electrodes added. They are composed of a voltage generator, the platinum electrode equivalent circuit and the cable model (Rs_{patch}, Rp_{patch} and C_{patch}), to connect the peripheral electrodes with the nerve fiber that we want to activate.

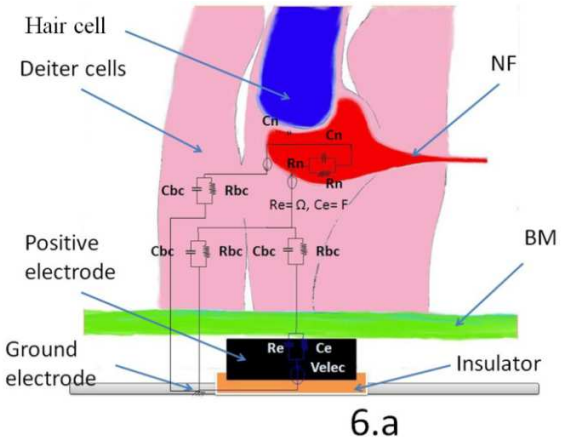

Figure 6.a. Electrical analog of the electrode and nerve.

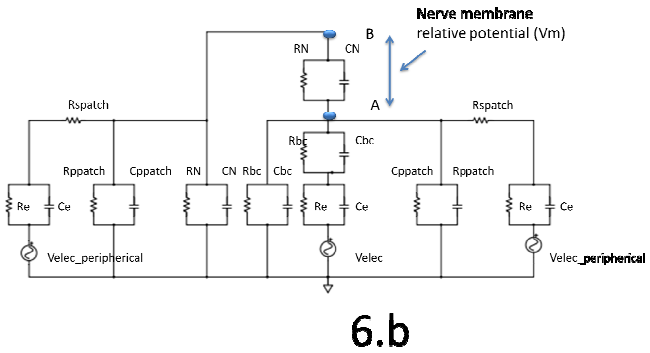

Figure 6.b. Electrical analog with three electrodes

The main goal of the addition of the two surrounding electrodes was to study theoretically the influence of these on the stimulation of selected nerve fibers (or more precisely of the packet of nerve fibers that should only be stimulated by the central electrode). These perturbations, if significant, could make the sound reconstitution inaccurate.

III. INTERPRETATION OF THIS ELECTRICAL ANALOG

The membrane potential (Vm) (which corresponds to the difference of potential between point A and point B in Figure 6.b) had to vary of 30mV to generate an AP. The electrode stimulation (Velec) was made using a DC source. Neglecting the effect of the capacitors, Vm varied linearly with Velec and the variation of 30mV was reached for an electrode stimulus around 0.9V.

When a nerve fiber is stimulated constantly, it will not produce an AP indefinitely but rather produce a succession of randomly spaced AP called spike trains. The spike train length that could be produced by a sound of given intensity has to be reproduced with the electrodes of the cochlear implant. We performed transient simulation including the capacitors effects by injecting a square voltage with a period of 150ms. This experiment was repeated for input square voltages varying from 1V to 5V (Figure 7.a). The aim of this simulation was to study if the voltage amplitude sent to the electrode would affect the spike train duration and starting time. Figure 7.b reveals that the delays for Vm potential to reach its maximum value were around 0.1µs, which were small compared to the duration of a nerve AP (few ms). This result pointed out that theoretically the electrode voltage magnitude had a very insignificant effect on the spike train duration. In addition, the recreated spike train starting time has negligible delay with the electrode stimulation starting time.

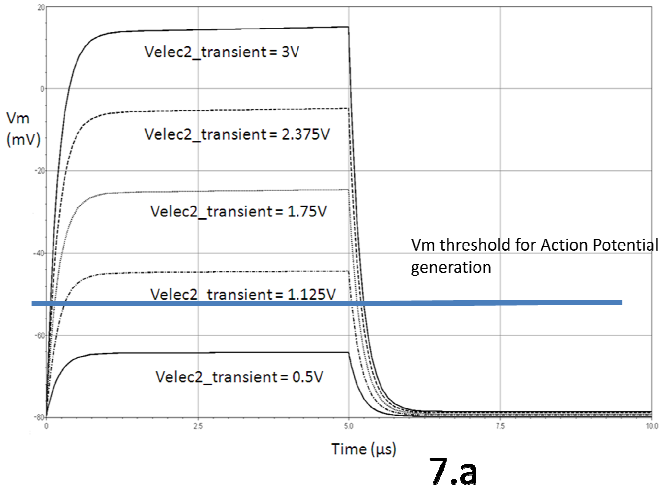

Figure 7.a. Transient simulation with different electrode voltage as input and Vm voltage as output.

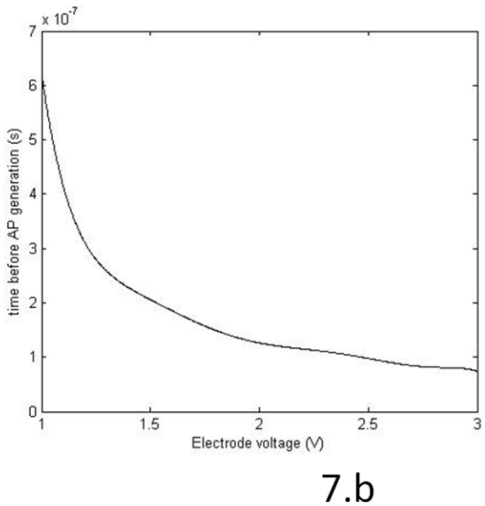

Figure 7.b. Time before AP generation depending on the elctrode voltage

A general overview of the spike train related to the Vm amplitude is presented in Figure 8. The AP generated were obtained from basic mathematical functions in order to model the

2014, © Copyright by authors, Published under agreement with IARIA - www.iaria.org

nerve fiber AP created after square voltage electrode stimulation. The interspike time was taken randomly and greatly depends on the amplitude of the stimulus [26]. However, the electrical analog presented in this paper does not account for this effect.

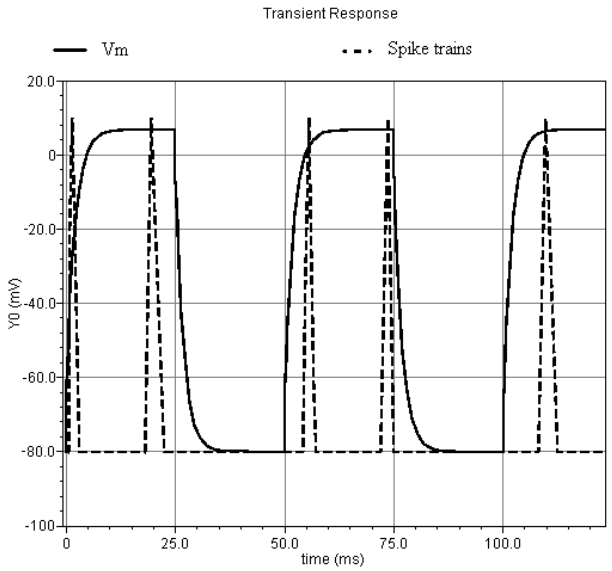

Figure 8. Spike train generated by the electrode input voltage

We performed also a parametric simulation using the electrical description of Figure 6.b, where the surrounding electrodes are added. The central electrode had a DC voltage of 1V and we varied the voltage of the surrounding electrodes between 0.9 and 5V. According to resistances and capacitances values used in Figure 6.b, analytical computation showed that when the voltage of the surrounding electrodes was maximum (5V), the nerve fibers (above the central electrode) membrane potential Vm variation was 0.5mV, which was not high enough to stimulate these nerve fibers (the ones that should be stimulated only by the central electrode).

The overall system consumption is a great significance as cochlear implants are not convenient for the user to recharge. The study of the power consumption is presented Figure 9.

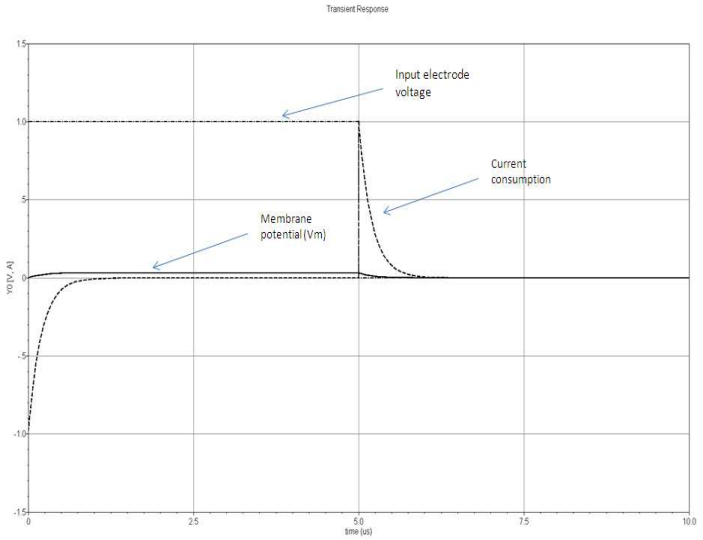

Figure 9. Current consumption during one stimulation period

The current peaks during each input signal transitions could reach 1A. Consequently, the maximum power consumed during a square input signal generation by the electrodes was around 1W (peak value), whereas the mean power consumed per period was around 50mW. These results may be used for the electrode array design to define battery size as well as electrode minimum width.

IV. NERVE REPARTITION MAP

The biomechanical most widespread theory of BM vibration is the Traveling Wave theory: following acoustic vibrations, the BM is excited and vibrates at a particular place inside the cochlea. This place depends on the sound wave frequency as well as sound amplitude [27], [28]. Cochlear implants aim to recreate the neural stimuli of an healthy cochlea using an wired electrodes array inserted inside the scala tympani, close to the BM. As each electrode is at a fixed place inside the cochlea, electrode stimulation will excite only a limited region of the cochlea which will be further interpreted in the brain as a sound of a certain frequency as indicated in Figure 10. Consequently, sound division into single frequency (using the Fast Fourier Transform (FFT) algorithm for instance) is necessary to select the right electrode to activate which then stimulates its surrounding nerve fibers.

In order to only select the nerve fibers associated with the resonating IHC, we created an afferent nerve fiber map of the cochlea including the frequency selective mechanisms of the ear.

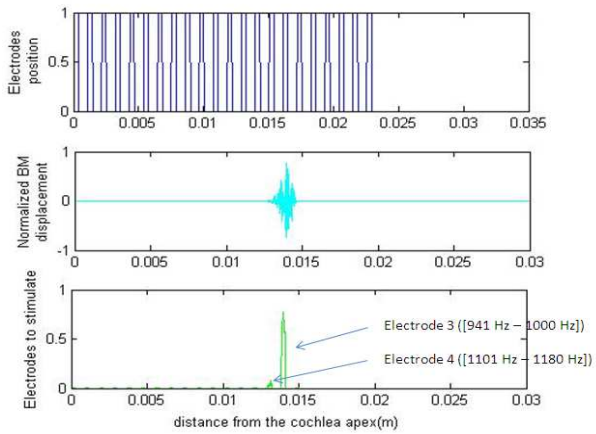

Figure 10. The auditory nerve fibers position stimulated by the electrodes array (a), BM displacement for a 1250Hz sine wave (b), Resulting electrodes stimulated by the 1250 Hz sine wave based on the BM displacement theory (c).

V. SPIRAL GANGLIONS

There are between 30000 to 40000 nerve fibers in the cochlea of a normal adult [29]. Three types of nerve fibers innervate the cochlea: autonomic, which are associated with blood vessel and other physiological functions, afferent (conducting information from the cochlea to the brain) and efferent (conducting information from the brain to the cochlea, especially to the Outer Hair Cells). Afferent nerve fibers are produced by Spiral Ganglions Cells (SGC) [30]. Spiral ganglions are synaptically connected to the IHC and OHC as indicated in Figure 11.

Type I SGC represent 95% of the SGC and each one connects to a single IHC whereas a single IHC is connected to 10-20 type I SGC [30].There are around 15 nerve fibers per IHC in the lower second turn of the cochlea and this number changes from the base

2014, © Copyright by authors, Published under agreement with IARIA - www.iaria.org

to the apex, most probably slightly contributing the cochlea sensitivity toward certain frequencies [31], [32], [33].

Type II spiral ganglions are smaller and unmyelinated and mostly connect OHC.

It may be deduced that IHC are surrounded by almost all the afferent nerve fibers, therefore, they are thought to function primarily as sensory receptors [34]. OHC otherwise are more connected with motor properties of the stereocilia [35], they may permit an higher accuracy in sound perception.

In [36], the spiral ganglions repartition over the cochlea distance from the base is presented for cats. We assumed that the spiral ganglions cochlea distribution for other terrestrial mammal species was similar [37], [38] (this assumption may be used as first approximation).

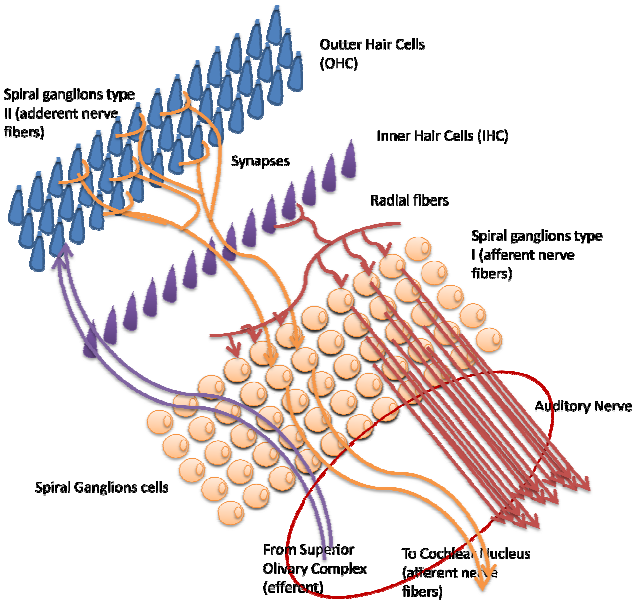

Figure 11. Auditory Nerve fibers and hair cells. Redrawn from [39]

As type II SGC function in hearing sensation has been partially understood and because their number is limited compared to type I SGC number, we neglected type II SGC, and supposed in this model that:

- the total SGC number and repartition was entirely defined by type I SGC.
- the total afferent nerve cell number and repartition inside the cochlea was therefore similar to type I SGC number and repartition.

VI. EAR FREQUENCY SENSITIVITY HYPOTHESIS

When the eardrum is stimulated, the nerve response over frequency presents a peak amplitude around 4KHz [40]. The human ear is composed of the outer ear, the medium ear and the inner ear (where BM makes the Organ of Corti oscillates) [41]. This particular human hearing frequency sensitivity may result from the combined effects of outer ear resonance, the middle ear resonance and the cochlea sound filtering and amplification.

It has been suggested that the outer ear and the medium ear contributes to frequency sensitivity in mammalian hearing, especially for frequencies around 3KHz [42], [43], [39], [44] [45].

The cochlea frequency sensitivity may also result from others various mechanisms still controversial. Considering only the cochlea biophysics, the intracochlear/eardrum magnitude of the scala tympani over frequency found in [46] may indicate varying vibrations amplitude depending on the sound wave frequency. The BM displacement, when stimulated by a mechanical wave, contributes to produce the frequency sensitivity of the cochlea due to the BM different physical properties (stiffness, etc.) inside the cochlea (distance from the base).

The cochlea sensitivity toward certain frequencies may be further affected by other physiological factors, such as different afferent nerve fibers repartition and stimulation, depending on the position on the cochlea. Several mechanisms have been proposed such as:

- IHCs frequency response (similar to a low pass filter with a resonating pulse around 10KHz) [47], [48]. The IHCs frequency response may result from different IHCs length inside the cochlea or to their stereocilia and cellular mechanical properties. Furthermore, gradient of IHC ionic channels along the cochlea length exist and increase the frequency hearing sensitivity of the cochlea [49]
- Spiral ganglions density increases slowly and linearly with the cochlea position with respect of the cochlea location hence spiral ganglions repartition is related to the frequency of the sound wave but fails to explain the 4KHz frequency peak (cf spiral ganglions frequency map, presented in Figure 13) [36], [46]

To the authors personal interpretation the frequency selectivity of the cochlea is greatly linked to biophysics of the cochlea, to IHCs potential change and repartition and ear/middle ear resonance rather than nerve fiber topography (as it failed to explain the amplification peak in the 3-4KHz range [46]).

VII. AFFERENT NERVE FIBERS REPARTITION INSIDE THE COCHLEA

As indicated in [29], the number of afferent nerve fibers in the cochlea is around 40000 and their effective stimulation is depending on the sound wave frequency. We hence decided to create an afferent nerve repartition map already including all the physical or anatomical mechanisms presented in Section V (that we called Afferent Nerve Fibers Repartition Map Including Ear Frequency Selection Mechanisms or MEFFRINAM map), in order to roughly define the number of afferent nerve fibers affected by a sound wave. This map presents great interest for cochlear implants application as the electrodes array are directly stimulating these nerve fibers and the outer/middle ear resonance, the BM variations depending on wave frequencies, the Organ of Corti selective mechanisms, etc. are bypassed in cochlear implants, making the use of this map fundamental to recreate a realistic hearing.

To develop this topographic map we took first the reverse function of the human hearing threshold over frequencies [16] to get the human ear sensitivity toward the frequencies.

By making this function linear (R(f)) and then reversing it ($I_R(f)$), it allowed us to estimate the cochlea sensitivity toward frequency. Transforming the $I_R(f)$ function into a probability density function ($P_{IR}(f)$) and multiplying it with the total number of afferent nerves in the cochlea ($Nb_{afferentnerves}$) resulted in the Afferent Nerve Fibers Repartition Map Including Ear Frequency Selection Mechanisms (MEFFRINAM map) of the cochlea as expressed in (4):

2014, © Copyright by authors, Published under agreement with IARIA - www.iaria.org

$$Threshold\ of\ hearing = 10\log|R(f)| \rightarrow 10\log|I_R(f)| = -10\log|R(f)|$$

$$P_{IRT}(f) = \frac{I_R(f)}{\int_{f_{min}}^{f_{max}} I_R(f)} Nb_{afferentnerves} \quad (4)$$

Where P_{IRT} (f) is the equivalent afferent nerve stimulated repartition map over the frequencies (f).

The Greenwood function [50] was used to pass from the resonant frequency into a position in the cochlea (between the base and the apex) [50]. Therefore $P_{IRT}(f)$ can be transformed into $P_{IRT}(d_A)$ where d_A is the distance from the apex as described in (5):

$$f = 165.4\,(10^{2.1\,d_A} - 1)$$
$$P_{IRT}(f) = P_{IRT}\left(165.4\,(10^{2.1\,d_A} - 1)\right) \quad (5)$$

According to Greenwood parameters for human ear fitting [50].

Figure 12 displays the afferent nerve fibers stimulated map including ear amplification mechanisms (MEFFRINAM map) compared to cochlea position. The comparison between the spiral ganglions topographic map (extracted from [36]) and the created topographic map is presented in Figure 13. Based on the assumptions presented in Section V, both maps have the same number of cells but these are differently affected over frequencies.

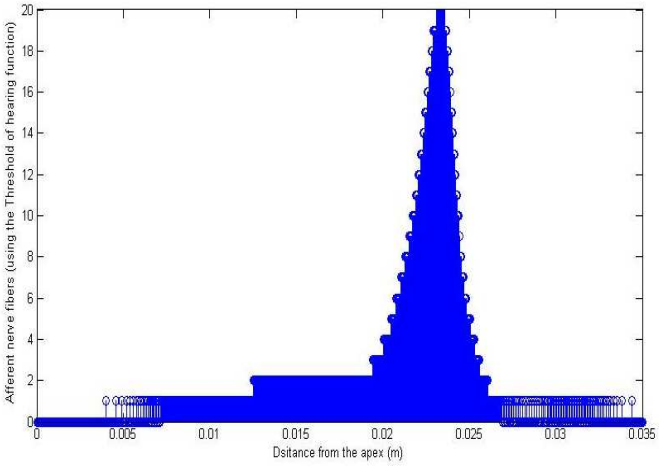

Figure 12. Afferent Nerve Fibers Repartition Map Including Ear Frequency Selection Mechanisms (MEFFRINAM map) in relation to the distance from the apex

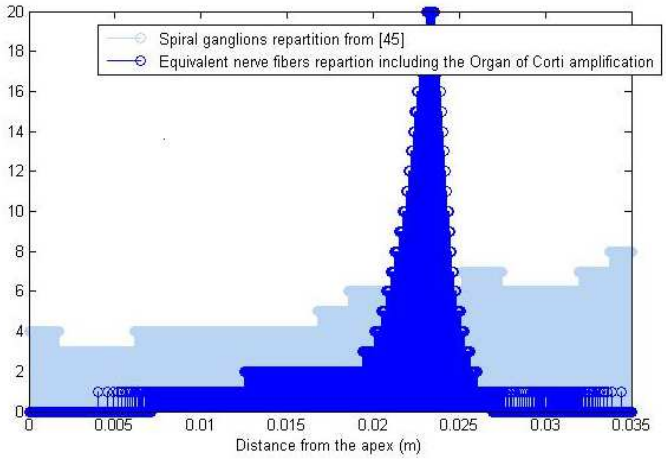

Figure 13. Comparison of spiral ganglions activation [36] and equivalent afferent nerve fibers stimulated map depending on the cochlea and ear biophysics (MEFFRINAM map in dark blue)

VIII. BENEFITS OF THE CREATED TOPOGRAPHIC MAP FOR COCHLEAR IMPLANTS

In severely deaf people the use of cochlear implants helps to partially recover the hearing function. In implanted patients the afferent nerve fibers stimulation is directly done through electrodes and does not require the Organ of Corti as explained in Section I. By remembering that we made the approximation that the afferent nerve fibers were equivalent to the SGC, the afferent nerve fibers selected by the electrodes is given by the spiral ganglions repartition map.

We use CI422 device characteristics with an insertion depth of 20-25mm, a mean diameter of the electrodes around 0.35mm and a spacing between the electrodes around 0.45mm. As explained in [23] the number of nerve fibers stimulated by an electrode is a function of the power magnitude as well as the proximity of the electrodes with the SGC.

We supposed that the electrodes are very close to the SGC, resulting in a window type selection (very accurate) of the afferent nerve fibers. In practice, this may be inexact as the insertion of the electrode array inside the scala tympani is difficult and usually result in spacing between the electrodes array and the Spiral ganglions [51] .In consequence, in practice, the nerve fibers selection mathematical description is closer to a Gaussian function.

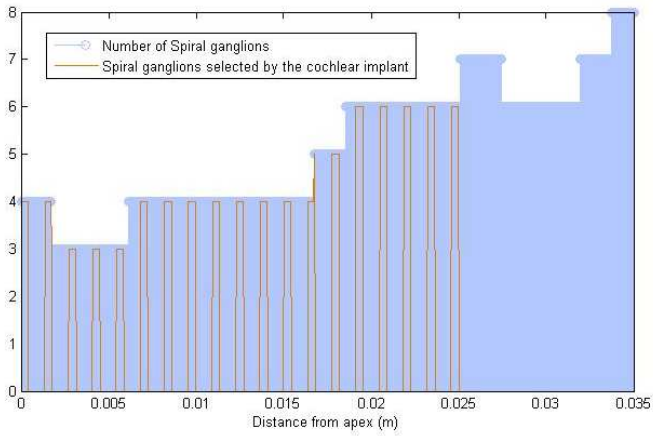

Figure 14. Packet of afferent nerve fibers selected by the electrodes of the cochlear implants

From Figures 13 and 14, it can be easily deduced that the cochlear implant electrodes do not provide the required amplification in the 2KHz – 6KHz frequency range as Cochlear amplification is not done. Algorithmic correction by modifying the energy sent to the electrodes may be used to correct this defective amplification. This algorithmic correction should be based on the human hearing threshold or similarly on the equivalent afferent nerve fibers stimulated map, which takes into consideration the amplification mechanisms of an healthy cochlea.

Using the mathematical logarithmic spiral representation presented in [52], the spatial representation of the cochlea can be performed. The mathematical equation in the cited document describes a flat spiral disagreeing with a real cochlea, however we may use the z direction to plot information such as the nerve fiber topographic map or those nerve fibers selected by the electrodes array, as indicated in Figures 15 and 16.

2014, © Copyright by authors, Published under agreement with IARIA - www.iaria.org

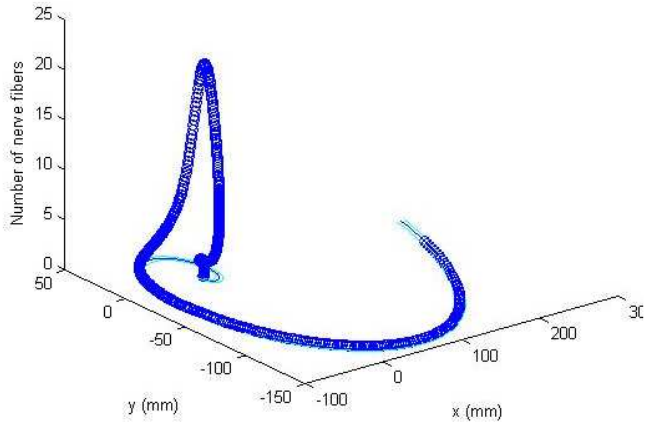

Figure 15. Afferent Nerve Fibers Repartition Map Including Ear Frequency Selection Mechanisms inside the cochlea depending on the cochlea spatial position

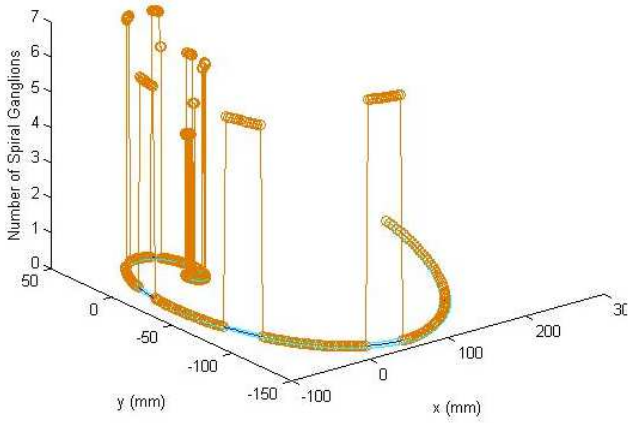

Figure 16. Portion afferent nerve fibers inside the cochlea stimulated by the cochlear implant electrodes

IX. AMPLIFICATION COEFFICIENTS ASSOCIATED WITH THE TOPOGRAPHIC MAPS COMPARISON

Cochlear implant electrodes should hence be multiplied by a scalar coefficient to correctly model the frequency sensitivity of the ear. This correction is compulsory as the Central Nervous System interprets neuronal signals already amplified in some particular frequencies. If the frequency amplitude dependence is not reproduced in cochlear implants it may result in inability to correctly hear certain frequencies (especially in the 3-4KHz band), ultimately resulting in sound distortion. Comparison between the MEFFRIMAM map and the Spiral Ganglions topographic map selected by the cochlear implants is exposed in Figure 17.

To correctly model the frequency response of an healthy ear, each electrode should be multiplied with the coefficient indicated in Figure 18. We further supposed that the number of nerve fibers stimulated is linearly increasing with the amplitude of the electrode. This may be inaccurate for high voltage stimulus or very low voltage stimulus due to saturation mechanisms [53], [54], [55].

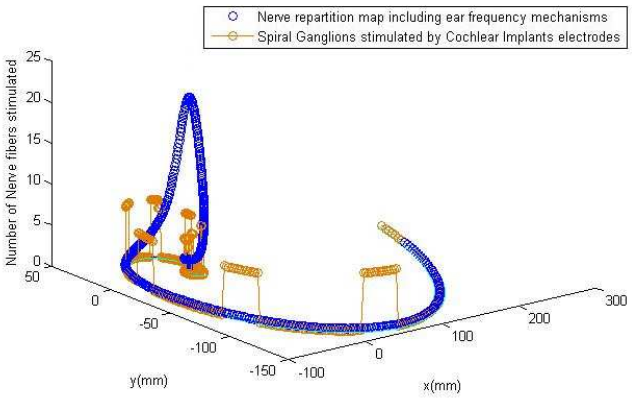

Figure 17. Comparison between the Spiral Ganglions stimulated by the electrodes and the created MEFFRIMAM map

To compute this average coefficient a simple division was performed between the afferent nerve fibers number in the MEFFRIMAM map and the afferent nerve fibers number defined by the spiral ganglions map for the same position inside the cochlea. The average value of this coefficient was retained for each electrode.

The multiplication of these coefficients with the voltage value that must be sent at an electrode to stimulate an afferent nerve fiber response (defined in Section III) could be done in the processing unit of the cochlear implant. Furthermore, coefficients amplitude tuning tests performed in deaf people using cochlear implants for each electrode may add precision in the hearing response of these patients.

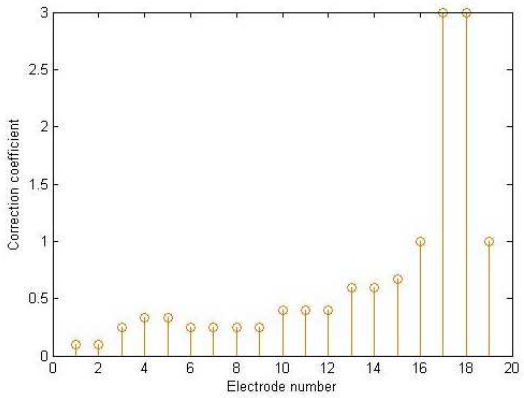

Figure 18. Electrodes amplification coefficients to ensure similar frequency response with an healthy cochlea

X. CONCLUSION

The theoretical electrical description presented in this paper was used to carry out simulations allowing the detection of the minimum voltage needed to ensure nerve fibers stimulation. This voltage was found around 0.9 V. Furthermore, the current peaks during each input signal transitions could reach 1A (peak value), and the mean power consumed per period was around 50mW. These results may be used as requirements for the electrode array design and corresponding control electronics.

It has also been suggested that two consecutive electrodes were not disturbing one another and that the duration of the stimulation did not depend on the input electrode voltage. A more complex model, including the spike trains frequency (which is

2014, © Copyright by authors, Published under agreement with IARIA - www.iaria.org

the number of spikes generated per second) related to the electrode input voltage is being currently developed.

Furthermore, using the threshold of hearing function, we created a topographic map of afferent nerve fibers repartition inside the cochlea weighted by the frequency selectivity of an healthy ear. This map may be of great value to decrease sound distortion in cochlear implants. Corrective coefficients were defined for each electrodes in order to allow electrode potential fine tuning based on the biophysical properties of the ear.

Besides physical tests are ongoing to ensure that the theoretical results obtained match the measurements. Deaf people using cochlear implants were asked to kindly submit themselves to cochlear implant reprogramming in order to test if the threshold of 0.9 V was sufficient; if not, it would greatly affect the perturbation between electrodes. We are also currently implementing the electrode potential correction algorithm in a portative platform in order to estimate its power consumption and facilitate its integration in cochlear implant device.

XI. REFERENCES

[1] U. Cerasani and W. Tatinian, "Modeling of the Organ of Corti Stimulated by Cochlear Implant Electrodes", CENTRIC 2013, The Sixth International Conference on Advances in Human oriented and Personalized Mechanisms, Technologies, and Services, pp. 80-85, 2013

[2] J. K. Niparko, Cochlear Implants: Principles and Practices (chapter 7). Lippincott Williams & Wilkins, 2009.

[3] G. Clark, Cochlear Implants: Fundamentals and Applications (ch. 4-8): Springer-Verlag, 2003.

[4] G. V. Békésy, Experiments in Hearing, part 3. Chap 12-14, 1989.

[5] F. N. F. Mammano, "Biophysics of the cochlea: linear approximation", J. Acoustic. Soc. Am. 93, vol. 6, June 1993.

[6] C. Kubisch *et al.*, "KCNQ4, a Novel Potassium Channel Expressed in Sensory Outer Hair Cells, Is Mutated in Dominant Deafness", Cell, vol. 96, issue 3, pp.437-446 February 1999.

[7] L. Trussel, "Mutant ion channel in cochlear hair cells", PNAS, vol. 97, issue 8, pp. 3786 –3788, April 2000.

[8] S. K. Griffiths. *INNER EAR.ppt*. [Online]. Available from: http://web.clas.ufl.edu/users/sgriff/A&P.html

[9] S. K. Juhn, B. A. Hunter and R. M. Odland, "Blood-Labyrinth Barrier and Fluid Dynamics of the Inner Ear", The internationnal tinnitus journal, vol. 7, issue 2, pp. 78-83, December 2001.

[10] R. Yehoash and R. A. Altschuler, "Structure and innervation of the cochlea", Elsevier, Brain Research Bulletin, vol. 60, pp. 397 - 422, January 2003.

[11] M. F. Bear, Neuroscience, Chapter 4, The Action Potential, ed. Baltimore: Lippincott Williams & Wilkins, 2007.

[12] A. Siegel and H. N. Sapru, Essential Neuroscience, Section II The Neuron, ed. Lippincott Williams & Wilkins, April 2010.

[13] K. X. Charand. *Action Potentials*. [Online]. Available from: http://hyperphysics.phy-astr.gsu.edu/hbase/biology /actpot.html

[14] A. Kral, D. Mortazavi and R. Klinke, "Spatial resolution of cochlear implants: the electrical field and excitation of auditory afferents", Hearing Research, vol. 121, pp. 11-28, 1998.

[15] L. Sileo *et al.*, "Electrical coupling of mammalian neurons to microelectrodes with 3D nanoprotrusions", Elsevier, Microelectronic Engineering, vol. 111, pp. 384–390, November 2013

[16] C. Fielding. *Lecture 007 in Hearing II*. [Online]. Available from: http://www.feilding.net/sfuad/musi3012-01/html/lectures/007_hearing_II.htm

[17] M. Hubin. *Propriétés des milieux biologiques*. [Online]. Available from: http://michel.hubin.pagesperso-orange.fr/capteurs/biomed/chap_b6.htm

[18] R. Nave. *Parallel Plate Capacitor*. [Online]. Available from: http://hyperphysics.phy-astr.gsu.edu/hbase/electric/pplate.html,

[19] P. Glover, *Resistivity theory*. [Online]. Available from: http://www2.ggl.ulaval.ca/personnel/paglover/CD%20Contents/GGL-66565%20Petrophysics%20English/Chapter%2017.PDF

[20] J. D. Bronzin, "The Electrical Conductivity of Tissues", in The Biomedical Engineering Handbook: Second Edition, ed. Myer Kutz, 2000.

[21] N. Ida, "9.2 electromagnetic properties of materials", in Engineering Electromagnetics, ed. Springer, 2003.

[22] Scitable by Nature. *Microtubules and Filaments*. [Online]. Available from: http://www.nature.com/scitable/topicpage/microtubules-and-filaments-14052932

[23] Cochlear®. *Delivering choice, cochlear's electrodes portofolio-as unique as our customers*. [Online]. Available from: www.cochlear.com

[24] J. Yang and J. B. Wang, "Morphological observation and electrophysiological properties of isolated Deiters' cells from guinea pig cochlea", NCBI Pubmed, vol. 14, issue 1, pp. 29-31, January 2000.

[25] A. L. Hodgkin and A. F. Huxley, "A quantitative description of membrane current and its application to conduction and excitation in nerve", The Journal of Physiology, vol. 117, issue 4, pp. 500-544, 1952.

[26] X. Wang. *Neural representation of Sensory stimuli: Properties of Spike trains*. [Online]. Available from: http://www.shadmehrlab.org/

[27] R. F. Lyon and C. A. Mead. *Cochlear Hydrodynamics demystified*. [Online]. Available from: Department of Computer Sciences, California Institute of Technology

[28] L. Watts. *Cochlear mechanics: Analysis and analog VLSI*. [Online]. Available from: California Institute of Technology

[29] E. L. Mancall and D. G. Brock, Gray's clinical neuroanatomy, ed. Elsevier Health Sciences, 2011.

[30] University of Rochester. *Auditory Nerve I, Innervation of the Cochlea Frequency & Level Coding*. [Online]. Available from: http://www.bcs.rochester.edu/courses/crsinf/221/ARCHIVES/S11/Auditory_Nerve1.pdf

[31] L. A. Werner. *The auditory nerve response*. [Online]. Available from: http://depts.washington.edu/

[32] R. Jonsson, "Field interactions in the peripheral auditory neural system with reference to cochlear implants",

2014, © Copyright by authors, Published under agreement with IARIA - www.iaria.org

Electrical, Electronic and Computer Engineering, University of Pretoria, 2011.

[33] A. F. Jahn and J. Santos-Sacchi, Physiology of the Ear, ed. Cengage Learning, 2001.

[34] M. Deol and S. Gluecksohn-Waelsch, "The role of inner hair cells in hearing", Nature, vol. 278, pp.250 - 252, 1979

[35] J. Zheng, W. Shen, D. Z. He, K. B. Long, L. D. Madison and P. Dallos, "Prestin is the motor protein of cochlear outer hair cells", Nature, vol. 405, pp. 149-155, 2000

[36] I. Chen, C. J. Limb, and D. K. Ryugo, "The effect of cochlear-implant-mediated electrical stimulation on spiral ganglion cells in congenitally deaf white cats", Journal of the Association for Research in Otolaryngology, vol. 11, pp. 587-603, 2010.

[37] Luisanna State University. *Hearig Range Animals*. [Online]. Available from: http://www.lsu.edu/deafness /HearingRange.html

[38] R. R. Fay, "Structure and function in sound discrimination among vertebrates", The evolutionary biology of hearing, ed. Springer, pp. 229-263, 1992

[39] Steven Errede. *The Human Ear Hearing, Sound Intensity and Loudness Levels*. [Online]. Available from: http://courses.physics.illinois.edu

[40] University of Illinois. *The Human Ear: Hearing, Sound Intensity and Loudness Levels*. [Online]. Available from: http://courses.physics.illinois.edu/phys406/Lecture_Notes/P406POM_Lecture_Notes/P406POM_Lect5.pdf

[41] P. W. Alberti. *The anatomy and physiology of the ear and hearing*. [Online]. Available from: http://www.who.int/occupational_health/publications/noise2.pdf

[42] D. Purves, G. J. Augustine, D. Fitzpatrick, L. C. Katz, A. S. LaMantia, J. O. McNamara, et al., The External Ear, Neuroscience Second Edition, ed. Sinauer Associates, 2001.

[43] S. S. Stevens and H. Davis, Hearing: Its psychology and physiology, ed.Wiley New York, 1938.

[44] University of Utah. *All about ears*. [Online]. Available from: Physics of the Human Body - Physics 3110

[45] University of Wisconsin. *IV. Functions And Pathphysiology Of The Middle Ear*. [Online]. Available from: Departement of Neurophysiology

[46] University of Vermont. *Coclia Anatomy and physiology of hearing*. [Online]. Available from: University of Vermont, College of Medicine

[47] University of Rochester. *Auditory Nerve I, Innervation of the Cochlea Frequency & Level Coding*. [Online]. Available from: http://www.bcs.rochester.edu/courses /crsinf/221/ARCHIVES/S11/Auditory_Nerve1.pdf

[48] P. Dallos, "Response characteristics of mammalian cochlear hair cells", The Journal of neuroscience, vol. 5, pp. 1591-1608, 1985.

[49] J. Ashmore, "Biophysics of the cochlea–biomechanics and ion channelopathies", British medical bulletin, vol. 63, pp. 59-72, 2002.

[50] D. D. Greenwood, "A cochlear frequency-position function for several species—29 years later", The Journal of the Acoustical Society of America, vol. 87, p. 2592, 1990.

[51] R. Shepherd, S. Hatsushika, G. M. Clark, "Electrical stimulation of the auditory nerve: the effect of electrode position on neural excitation", Hearing research, vol. 66, pp. 108-120, 1993.

[52] K. Cheng, V. Cheng, and C. H. Zou, "A logarithmic spiral function to plot a Cochleaogram", Trends in Medical Research, vol. 3, pp. 36-40, 2008.

[53] S. J. Elliott and C. A. Shera, "The cochlea as a smart structure", Smart Materials and Structures, vol. 21, pp. 064001, 2012.

[54] R. Zelick. *Vertebrate Hair Cells*. [Online]. Available from: http://web.pdx.edu/~zelickr/sensory-physiology /lecture-notes/OLDER/L12b-hair-cells.pdf

[55] A. W. Peng, F. T. Salles, B. Pan, and A. J. Ricci, "Integrating the biophysical and molecular mechanisms of auditory hair cell mechanotransduction", Nature communications, vol. 2, pp. 523, 2011.

2014, © Copyright by authors, Published under agreement with IARIA - www.iaria.org